applied optics

Variable step size adaptive cuckoo search optimization algorithm for phase diversity

Dequan Li,[1,2,*] Shuyan Xu,[1] Xin Qi,[1,2] Dong Wang,[1] and Xiaotao Cao[1]

[1]Space Optics Department, Changchun Institute of Optics, Fine Mechanics and Physics, Chinese Academy of Sciences, Changchun, Jilin 130033, China
[2]University of Chinese Academy of Sciences, Beijing 100049, China
*Corresponding author: lidequan@ciomp.ac.cn

Received 9 August 2018; revised 26 August 2018; accepted 31 August 2018; posted 4 September 2018 (Doc. ID 341910); published 25 September 2018

The phase diversity (PD) algorithm will eventually be converted into a large-scale nonlinear numerical optimization problem, so the selection of numerical optimization algorithm will directly determine the accuracy and speed of the algorithm settlement. In this paper, we introduce the cuckoo search optimization algorithm, which has the advantages of simple model, few parameters, and easy implementation, to the phase diversity algorithm. By improving the step size control factor in the original cuckoo search algorithm, we can make it have faster optimization speed for PD. In the simulation experiments, we further proved and gave a simple explanation in theory that in the case of large-scale wavefront sensing, compared to the traditional particle swarm algorithm, this improved algorithm has higher accuracy and faster convergence speed. Finally, we set up a simple experimental system and proved the effectiveness of the improved cuckoo search algorithm for PD.

OCIS codes: (010.7350) Wave-front sensing; (100.5070) Phase retrieval; (100.3010) Image reconstruction techniques; (000.3860) Mathematical methods in physics.

https://doi.org/10.1364/AO.57.008212

1. INTRODUCTION

Wavefront sensing is an important part of active optics and adaptive optics systems. There are many commonly used wavefront detection methods. Some methods depend on the hardware facilities [1–4] and others are based on images [5–7]. In these methods, the phase diversity (PD) algorithm has the advantages of simple optical path, no special requirements for optical devices, and no additional sensors. In recent years, it has gained many applications [8–10].

The phase diversity algorithm will eventually be converted into a large-scale nonlinear numerical optimization problem. Therefore, how to choose an effective numerical optimization algorithm determines the accuracy and speed of the final aberration solution. The commonly used numerical optimization algorithms include particle swarm optimization [11], back propagation neural network [12,13], genetic algorithm [14], and Broyden–Fletcher–Goldfarb–Shanno (BFGS) [15].

The traditional particle swarm optimization algorithm needs to establish a balance between diversification and centralization; otherwise, it is easy to fall into the local optimum. Although there have been related papers to solve this problem, the number of Zernike polynomials in the phase diversity algorithm cannot be too much. The training time of the neural network algorithm is generally longer, and the accuracy of the training sample is generally difficult to guarantee. The traditional BFGS method converges only when the evaluation function is a convex function, and the calculation time is longer, which requires a higher computational burden.

Synthesizing the above questions, this paper proposes the use of the cuckoo search (CS) optimization algorithm [16–18] to solve the large-scale nonlinear optimization problem in the phase diversity algorithm. The optimization algorithm has the advantages of simple model, few parameters, and easy implementation. And the algorithm has higher settlement accuracy with faster convergence speed when the dimension of the optimization parameter is higher.

To improve the convergence rate of cuckoo algorithms, this paper proposes a variable step size adaptive cuckoo optimization algorithm based on the traditional cuckoo algorithm, which improves the step size control factor, and applies it to the phase diversity algorithm.

2. PHASE DIVERSITY TECHNIQUE

The phase diversity algorithm was proposed by Gonsalves in 1982 [19]. The main goal of PD is to reconstruct the wavefront aberration of the focal optical system by building an optimization problem.

The relations of the focus image collected in the focus surface and the object in the spatial domain in this optical system are

$$i(x,y) = o(x,y) * \mathrm{PSF}(x,y), \tag{1}$$

and the relationship in the frequency domain is

$$I(u,v) = O(u,v) \bullet \mathrm{OTF}(u,v). \tag{2}$$

And PSF(u,v) can be obtained by the inverse Fourier transform of generalized pupil function:

$$\mathrm{PSF}(u,v) = |\mathrm{FT}^{-}(P(x,y))|^2. \tag{3}$$

In the above equation, the variables x, y are all variables in the spatial domain. $o(x,y)$ is the distribution function of the two-dimensional object. $i(x,y)$ is the intensity distribution of the image on the ideal focal plane. PSF(x,y) is the optical system point spread function corresponding to the intensity distribution of an ideal focal plane image. $P(x,y)$ is the generalized pupil function for an optical system. FT^{-}() is a two-dimensional inverse Fourier transform operation.

The pupil function of the optical system can be represented by the modulus value $A(x,y)$ and the phase $\phi(x,y)$. The equation is

$$P(x,y) = A(x,y)\exp(i\phi(x,y)). \tag{4}$$

Assuming that the pupil of the optical system is an ideal pupil, the module value is in the range of $\sqrt{x^2+y^2} \le D$, $A(x,y) = 1$; the module value is in the range of $\sqrt{x^2+y^2} > D$, $A(x,y) = 0$. In the equation, $\phi(x,y)$ is the unknown wavefront aberration. The phase diversity function can be developed by a Zernike polynomial with orthogonality in the unit circle [20]:

$$\phi(\rho,\theta) = \sum_{i}^{N} a_i c_i(\rho,\theta), \tag{5}$$

where N is the number of items of the selected Zernike polynomial expansion item. The coefficients $c_1 - c_3$ stand for piston, tip, and tilt of the wavefront aberration, which have no effect on the quality of the image, so in this article we do not consider $c_1 - c_3$.

Similarly, the relations of the defocus image collected in the defocus surface and the object in the spatial domain in this optical system are

$$i_d(x,y) = o(x,y) * \mathrm{PSF}_d(x,y), \tag{6}$$

and the relationship in the frequency domain is

$$I_d(u,v) = O(u,v) \bullet \mathrm{OTF}_d(u,v), \tag{7}$$

$$\mathrm{PSF}_d(u,v) = |\mathrm{FT}^{-}(P_d(x,y))|^2, \tag{8}$$

$$P_d(x,y) = A(x,y)\exp\, i(\phi(x,y) + \phi_d(x,y)). \tag{9}$$

In the above equation, $\phi_d(x,y)$ is the known defocus amount introduced, which can be represented by the fourth term representing the defocus amount in the Zernike polynomial:

$$\phi_d(x,y) = a_4 c_4(\rho,\theta). \tag{10}$$

The evaluation function is defined according to the maximum likelihood theory [21] to evaluate the degree of correlation between the reconstructed image and the actual image. The evaluation function's expression is given by Eq. (11),

$$E(o,a) = [i(x,y) - o(x,y) * \mathrm{PSF}(x,y)]^2 + [i_d(x,y) - o(x,y) * \mathrm{PSF}_d(x,y)]^2, \tag{11}$$

according to Parseval theory and convolution theory,

$$E(O,a) = [I(u,v) - O(u,v)\mathrm{OTF}(u,v)]^2 + [I_d(u,v) - O(u,v)\mathrm{OTF}_d(u,v)]^2, \tag{12}$$

under the following conditions:

$$\frac{\delta E(O,a)}{\delta O} = 0, \tag{13}$$

and further derivation

$$E(a) = \sum_{u\in X, V\in Y} \frac{|I(u,v)\mathrm{OTF}_d(u,v) - I_d(u,v)\mathrm{OTF}(u,v)|^2}{|\mathrm{OTF}(u,v)|^2 + |\mathrm{OTF}_d(u,v)|^2}. \tag{14}$$

3. MODIFIED CUCKOO SEARCH ALGORITHM

A. Review of the Traditional Cuckoo Search Algorithm

The CS algorithm is a swarm intelligence algorithm proposed by Yang in 2008 [22]. This algorithm is based on the obligate brood parasitic behavior of some cuckoo species in combination with the Lévy flight behavior of some birds and fruit flies. In recent years, due to its advantages such as simple model, few parameters, and easy implementation, it has been widely used in various numerical optimization problems.

The way in which cuckoos in nature choose to lay eggs is random or similar. When simulating the spawning method of cuckoo nests, we need to hypothesize the following three ideal states:

(1) The cuckoo only produces one egg at a time, and hatches with randomly selected bird nests.
(2) The most suitable nest position in each randomly selected nest position is reserved for the next generation.
(3) The number of bird nests is fixed at n, and the owner of the nest finds the exotic eggs with probability of $p_a \in [0,1]$. In this case, the host bird can either get rid of the egg, or simply abandon the nest and build a completely new nest.

On the basis of these three ideal states, the basic steps of CS can be summarized as follow [23]:

(1) Initialize the cuckoo search algorithm parameters.
The parameters consist of the number of nests (n), the discovering probability (pa) and the stopping criterion.
(2) Generate initial nests or eggs of host birds.
The initial locations of the nests are determined by the set of values randomly assigned to each decision variable as

$$x_{i,j}^{(0)} = \mathrm{round}[x_{j,\min} + \mathrm{rand}(x_{j,\max} - x_{j,\min})], \tag{15}$$

where $x_{i,j}^{(0)}$ determines the initial value of the jth variable for the ith nest; $x_{j,\min}$ and $x_{j,\max}$ are the minimum and the maximum allowable values for the jth variable; and rand is a random number in the interval [0,1]. The rounding function is accomplished due to the discrete nature of the problem.

(3) Generate new nests via Lévy flights.

In this step, all the nests except for the best one are replaced based on quality by new cuckoo eggs produced with Lévy flights from their positions as

$$x_i^{(t+1)} = x_i^{(t)} + a_0 S(x_i^{(t)} - x_{\text{best}}^{(t)})\text{rand}. \tag{16}$$

In the equation, x_i^t indicates that the ith nest is in the nest position of the tth generation. a_0 indicates the amount of step control, which is usually taken as 0.01, which x_{best}^t is the optimal solution of the tth generation nest positions. rand is a random number from a standard normal distribution, S is a random walk based on the Lévy flights. The Lévy flight essentially provides a random walk while the random step length is drawn from a Lévy distribution.

In the algorithm of Manategna [24],

$$s = \frac{\mu}{|\nu|^{1/\beta}}, \tag{17}$$

where u and v follow the standard normal distribution:

$$u \sim N(0, \sigma_u^2), \qquad \nu \sim N(0, \sigma_\nu^2), \tag{18}$$

$$\sigma_u = \left\{ \frac{\Gamma(1+\beta)\sin(\pi\beta/2)}{\Gamma[(1+\beta)/2]\beta 2^{(\beta-1)/2}} \right\}^{1/\beta}, \qquad \sigma_\nu = 1. \tag{19}$$

Lévy flights are more efficient than Brownian random walks in exploring unknown, large-scale search space. There are many reasons to explain this efficiency, and one of them is due to the fact that the variance of Lévy flights,

$$\sigma^2(t) \sim t^{3-\beta}, \qquad 1 \le \beta \le 2, \tag{20}$$

increases much faster than the linear relationship (i.e., $\sigma^2(t) \sim t$.) of Brownian random walks. This also provides a theoretical basis for higher ability of the cuckoo algorithm to solve high-dimensional problems than the traditional particle swarm algorithm.

(4) Alien eggs discovery.

After updating by location, contrast random numbers $r \in [0, 1]$ and p_a, if $r > p_a$, build new ones at new locations via Lévy flights. Finally, keep a group of bird nests $y_i^{(t+1)}$ with better test values, still remembered as x_i^{t+1}.

The CS can be summarized as the pseudo code shown in Fig. 1.

B. Variable Step Size Adaptive Cuckoo Search Algorithm

The step size of the position update in the CS algorithm is a random move in combination with the special Lévy flight of birds and fruit flies. When moving, the smaller the step, the slower the convergence rate, and the easier it is to fall into the local optimum solution. The larger the step, the faster the convergence speed is, and the easier it is to jump off the local optimal value and oscillate at the global optimal value. Because the step size generated by Lévy flight is random, it lacks adaptability. In order to improve the adaptability of the algorithm, inspired by the self-adaptation idea proposed in the literature when studying the particle swarm algorithm, this chapter uses the step-length factor update formula to replace the original a_0, so as to improve the CS algorithm. The improved algorithm is called the variable step size adaptive cuckoo search algorithm (VSACS).

begin
Objective function $f(x)$, $x = (x_1, \ldots, x_d)^{\mathrm{T}}$
Generate initial population of
n *host nests* $x_i (i = 1, 2, \ldots, n)$
while (t <MaxGeneration) *or (stop criterion)*
Get a cuckoo randomly by Lévy flights
evaluate its quality/fitness F_i
Choose a nest among n *(say,* j*) randomly*
if ($F_i < F_j$),
replace j *by the new solution;*
end
A fraction (p_a*) of worse nests*
are abandoned and new ones are built;
Keep the best solutions
(or nests with quality solutions);
Rank the solutions and find the current best
end while
end

Fig. 1. Pseudo code of the cuckoo search algorithm.

p is an integer greater than 1, in the range [1,30]. Draw the curve of a_0 is a function of $t/T_{\max}$, when p is taken as 1, 3, 5, 10, 20, and 30, respectively. t is the current number of iterations and $T_{\max}$ is the specified maximum number of iterations. The curve is shown in Fig. 2.

The improved algorithm flow is shown in Fig. 3.

The step size update equation is

$$a_0 = \exp(-30 \times (t/T_{\max})^p). \tag{21}$$

The step size factor a_0 of the bird nest position update gradually decreases as the number of iterations t increases. During the initial iteration of the algorithm, a large step length factor is maintained so that the algorithm can quickly converge to the position near the global optimal bird's nest. At the same time, the algorithm is prevented from falling into the local optimum. As the number of iterations increases, the step size gradually decreases. In the later stage of operation, the algorithm transforms into a local search and performs a finer search near the global optimal position. This makes the CS algorithm more adaptive and the number of iterations is significantly reduced. The value of p will be explained in the next section.

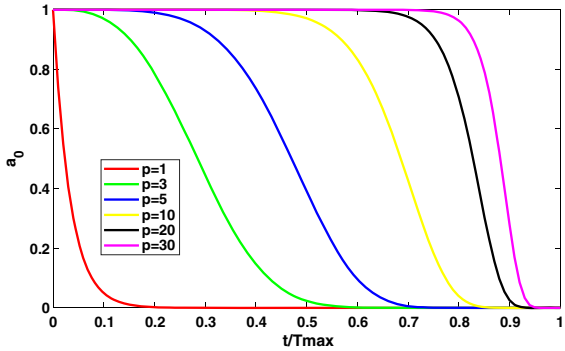

Fig. 2. Curve of a_0 is a function of $t/T_{\max}$.

begin
Objective function $f(x)$, $x = (x_1, \ldots, x_d)^{\mathrm{T}}$
Generate initial population of
n *host nests* $x_i (i = 1, 2, \ldots, n)$
while *(t <MaxGeneration) or (stop criterion)*
Calculate the step length control factor according to the formula (21)
Get a cuckoo randomly by Lévy flights
evaluate its quality/fitness F_i
Choose a nest among n *(say,* j*) randomly*
if $(F_i < F_j)$,
replace j *by the new solution;*
end
A fraction (p_a*) of worse nests*
are abandoned
calculate the step length control factor according to the formula (21)
new ones are built;
Keep the best solutions
(or nests with quality solutions);
Rank the solutions and find the current best
end while
end

Fig. 3. Pseudo code of improved cuckoo search algorithm.

4. NUMERICAL SIMULATION

A. Simulations of VSACS with Different p

In this section, a number of vast numerical simulations are processed to choose best value of p in the VSACS.

We randomly introduce 100 sets of coefficients within a certain range. For each set of aberration coefficients, we can use them to generate the in-focus and defocus point-spread function (PSF) images with Fourier optics.

Below we will use the VSACS with $p = 5$, $p = 15$, and $p = 30$ for PD, and give the root mean square error of calculated Zernike coefficients and true Zernike coefficients in the same number of iterations, which is expressed as Eq. (22), where n is the number of the aberration coefficients considered, c_i^t are the ith true aberration coefficients, and c_i^r are the nth calculated aberration coefficients:

$$\mathrm{RMSE} = \left\{ \frac{\sum_{i=4}^{n+4-1} (c_i^t - c_i^r)^2}{n} \right\}^{1/2}. \tag{22}$$

Table 1. Mean RMSE of the True Zernike Coefficients and the Calculated Zernike Coefficients of VSACS for PD with Different p under Two Different Conditions

Range (λ)	±0.25	±0.25
Zernike Size	7	12
$p = 5$	1.140e − 05	2.173e − 05
$p = 15$	4.350e − 06	1.763e − 05
$p = 30$	3.386e − 06	1.125e − 05

In the VSACS, discovering probability $p_a = 0.25$. The number of nests is 20 [16,18]. $\lambda = 632$ nm and $\phi_d(x, y) = \lambda$.

(a) The number of Zernike polynomials is 7 (c4–c10 of the fringe Zernike coefficients), and the range of aberration coefficients is $[-0.25\lambda, 0.25\lambda]$. The maximum number of iterations is 200.
(b) The number of Zernike polynomials is 12 (c4–c15 of the fringe Zernike coefficients), and the range of aberration coefficients is $[-0.25\lambda, 0.25\lambda]$. The maximum number of iterations is 1500.

As can be seen from Fig. 4 and Table 1, in the two cases, it can be seen that the RMSE of the VSACS with $p = 30$ for PD is significantly lower than others, so the p of VSACS is chosen to be 30 in this article.

B. Simulations of VSACS and CS

In this section, a number of vast numerical simulations are processed to verify the effectiveness and accuracy of the algorithm of VSACS than CS.

We randomly introduce 100 sets of coefficients within a certain range. For each set of aberration coefficients, we can use them to generate the in-focus and defocus PSF images with Fourier optics.

First, we give the number of iterations of the traditional cuckoo search algorithm for PD and variable step size adaptive cuckoo search algorithm for PD when the value of evaluation function Eq. (14) is less than 0.001 under the following different conditions. In the following cases, $\lambda = 632$ nm and $\phi_d(x, y) = \lambda$.

In the VSACS and CS, discovering probability $p_a = 0.25$ and $p = 30$ [16,18]. For easy comparison, the number of nests of the VSACS is the same as the number of nests of the CS. The number of nests is 20 [16,18].

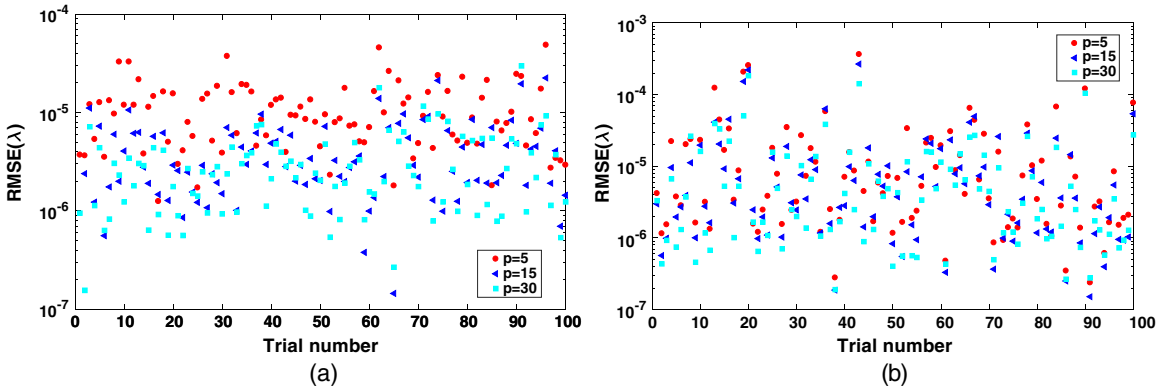

Fig. 4. Root mean square error of the true Zernike coefficients and calculated Zernike coefficients of VSACS for PD with different p under different conditions. In (a), the range of aberration coefficients to be searched is $[-0.25\lambda, 0.25\lambda]$, and the dimension is 7. In (b), the range of aberration coefficients to be searched is $[-0.25\lambda, 0.25\lambda]$, and the dimension is 12.

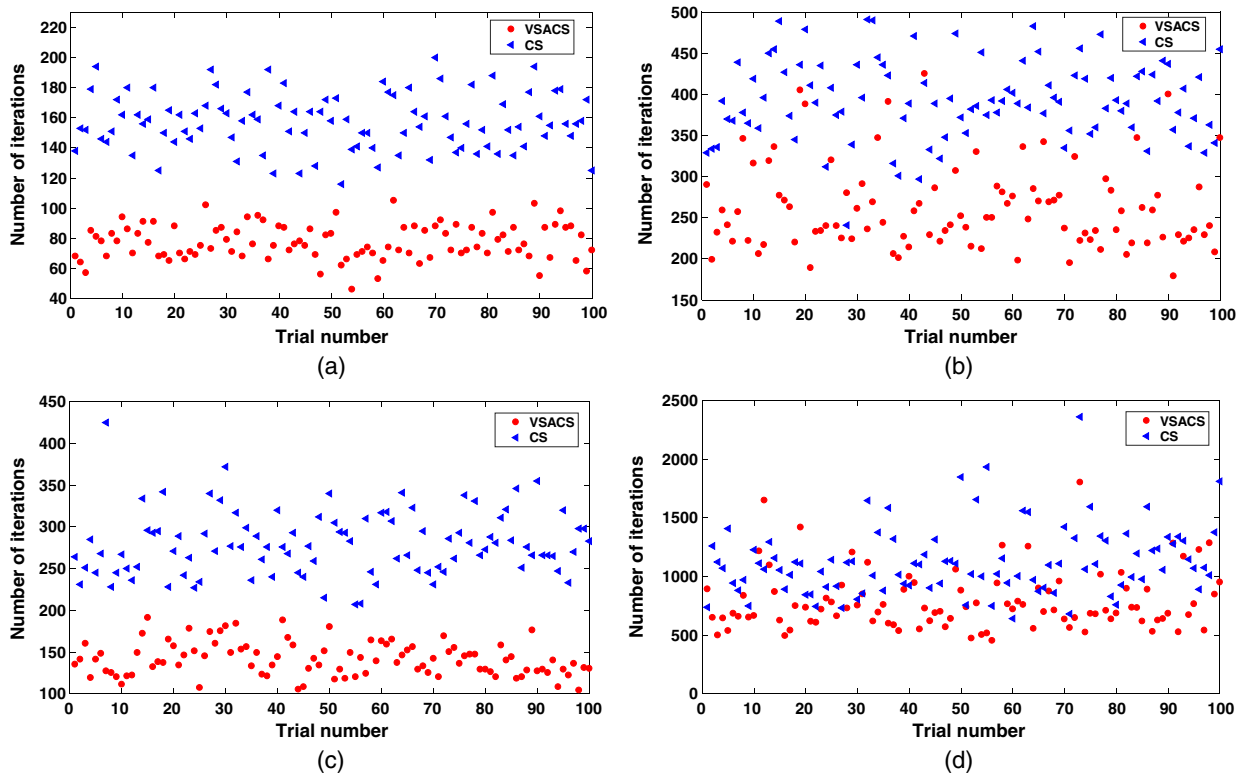

Fig. 5. Number of iterations of CS for PD and VSACS for PD when the evaluation function Eq. (14) value is less than 0.001 under different conditions. In (a), the range of aberration coefficients to be searched is $[-0.25\lambda, 0.25\lambda]$, and the dimension is 7. In (b), the range of aberration coefficients to be searched is $[-0.25\lambda, 0.25\lambda]$, and the dimension is 12. In (c), the range of aberration coefficients to be searched is $[-0.5\lambda, 0.5\lambda]$, and the dimension is 7. In (d), the range is $[-0.5\lambda, 0.5\lambda]$, and the dimension is 12.

(a) The number of Zernike polynomials is 7 (c4–c10 of the fringe Zernike coefficients), and the range of aberration coefficients is $[-0.25\lambda, 0.25\lambda]$.
(b) The number of Zernike polynomials is 12 (c4–c15 of the fringe Zernike coefficients), and the range of aberration coefficients is $[-0.25\lambda, 0.25\lambda]$.
(c) The number of Zernike polynomials is 7 (c4–c10 of the fringe Zernike coefficients), and the range of aberration coefficients is $[-0.5\lambda, 0.5\lambda]$.
(d) The number of Zernike polynomials is 12 (c4–c15 of the fringe Zernike coefficients), and the range of aberration coefficients is $[-0.5\lambda, 0.5\lambda]$.

As can be seen from Fig. 5 and Table 2, in the four cases, when the value of the evaluation function Eq. (14) is less than 0.001, the number of iterations of the VSACS is significantly less than the CS, so the VSACS algorithm has faster convergence speed, and the improvements to a_0 are effective.

Table 2. In the Four Cases, the Average Number of Iterations of CS and VSACS When the Value of Evaluation Function Eq. (14) Value Is Less Than 0.001

Range	$[-0.25\lambda, 0.25\lambda]$		$[-0.5\lambda, 0.5\lambda]$	
Zernike Size	7	12	7	12
CS	157.29	393.14	279.67	1126.02
VSACS	77.41	261.44	141.19	788.03

C. Simulations of VSACS and PSO

Compared to other population-based population algorithms, the VSACS has a higher solution accuracy and a faster solution speed in the case of large-scale wavefront sensing. This is because VSACS has two search capabilities [25]: local search and global search, controlled by a switching/discovery probability. The local search is very intensive with about 1/4 of the search time (for $p_a = 0.25$), while the global search takes about 3/4 of the total search time. This allows the search space to be explored more efficiently on the global scale, and consequently the global optimality can be found with a higher probability.

We still randomly introduce 100 sets of coefficients within a certain range. For each set of aberration coefficients, we can use them to generate the in-focus and defocus PSF images with Fourier optics.

Below we will use the VSACS for PD, the particle swarm optimization (PSO) for PD, and give the root mean square error of calculated Zernike coefficients and true Zernike coefficients in the same number of iterations, which is expressed as Eq. (22). $\lambda = 632$ nm and $\phi_d(x, y) = \lambda$. The maximum number of iterations is 1500.

In this paper, the "traditional PSO algorithm" particularly refers to the variant of the PSO algorithm proposed by Clerc [26], for this variant seems more widely applied at present.

In the traditional PSO algorithm, the learning factors $c1$ and $c2$ are usually set as $c1 = c2 = 2.05$ [11,27]. The population size is 40, and $w = 0.7298$.

Table 3. Mean RMSE of the True Zernike Coefficients and the Calculated Zernike Coefficients of VSACS for PD, PSO for PD under Four Different Conditions

Range (λ)	±0.1	±0.25	±0.35	±0.5
Zernike Size	24	20	16	12
PSO	1.101e – 02	6.762e – 02	5.340e – 02	0.303e – 01
VSACS	0.190e – 02	7.065e – 04	1.500e – 03	0.295e – 06

In the VSACS, discovering probability $p_a = 0.25$ and $p = 30$ [16,18]. For easy comparison, the number of nests is the same as the population size of the traditional PSO algorithm; the number of nests is 40.

(a) The number of Zernike polynomials is 24 (c4–c27 of the fringe Zernike coefficients), and the range of aberration coefficients is $[-0.1\lambda, 0.1\lambda]$.
(b) The number of Zernike polynomials is 20 (c4–c23 of the fringe Zernike coefficients), and the range of aberration coefficients is $[-0.25\lambda, 0.25\lambda]$.
(c) The number of Zernike polynomials is 16 (c4–c19 of the fringe Zernike coefficients), and the range of aberration coefficients is $[-0.35\lambda, 0.35\lambda]$.
(d) The number of Zernike polynomials is 12 (c4–c15 of the fringe Zernike coefficients), and the range of aberration coefficients is $[-0.5\lambda, 0.5\lambda]$.

In Table 3, the mean RMSE is the average RMSE of 100 sets of experiments.

From Fig. 6 and Table 3, it can be seen that the RMSE of the VSACS for PD is significantly lower than that of PSO for PD under the different conditions. This shows that the VSACS for PD has a stronger solving ability in the case of a high solution dimension, benefiting from the variance of Lévy flights increasing much faster than the linear relationship of Brownian random walks.

In a large number of simulation experiments, we found that the VSACS has a higher probability of finding the global optimum solution than the PSO algorithms. The specific experimental data of this phenomenon will not be given here. We will explore this phenomenon further in the future work.

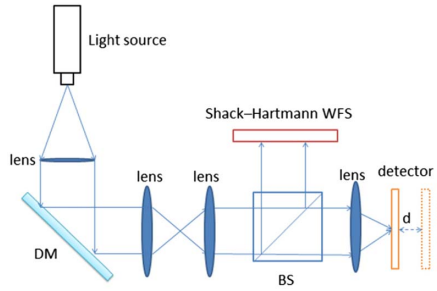

Fig. 7. Simplified block diagram of the experiment system of PD.

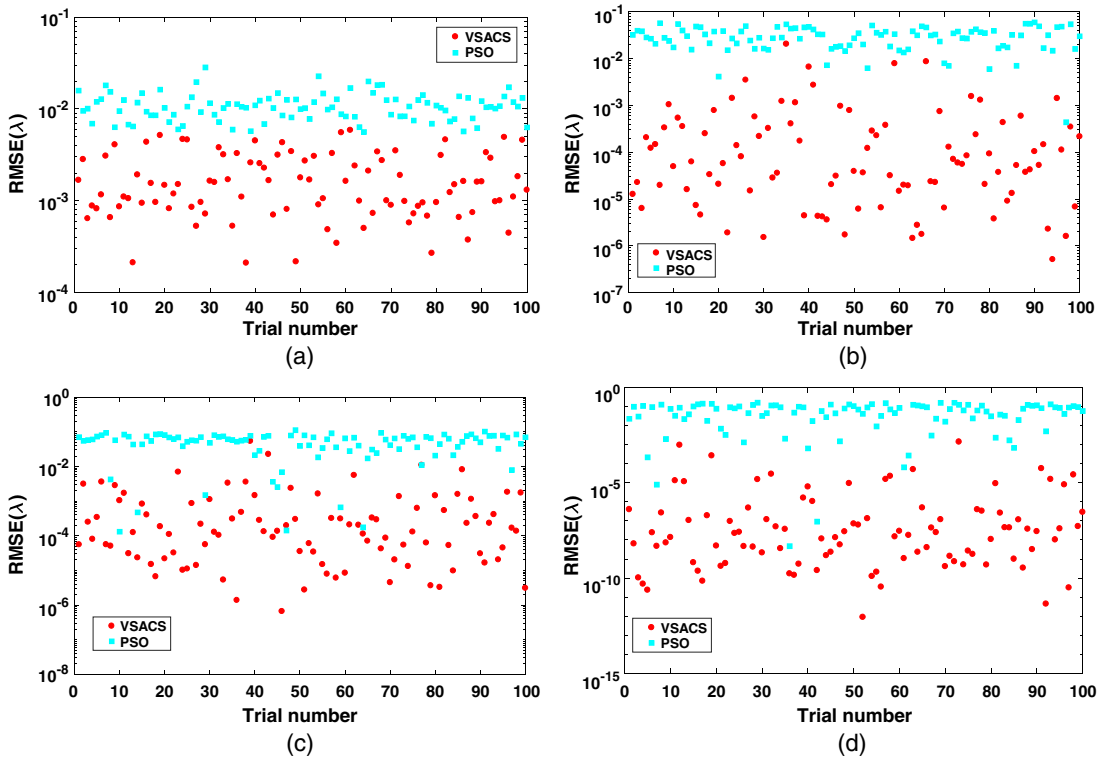

Fig. 6. Root mean square error of the true Zernike coefficients and calculated Zernike coefficients of VSACS for PD, and PSO for PD under different conditions. In (a), the range of aberration coefficients to be searched is $[-0.1\lambda, 0.1\lambda]$, and the dimension is 24. In (b), the range of aberration coefficients to be searched is $[-0.25\lambda, 0.25\lambda]$, and the dimension is 20. In (c), the range of aberration coefficients to be searched is $[-0.35\lambda, 0.35\lambda]$, and the dimension is 16. In (d), the range of aberration coefficients to be searched is $[-0.5\lambda, 0.5\lambda]$, and the dimension is 12.

5. EXPERIMENT

In order to further verify the effectiveness of the VSACS for PD, we conducted a simple experiment. A simplified block diagram of the verification experiment system of PD is shown in Fig. 7, and the real facility of the optical system is shown in Fig. 8.

The detector is installed in a one-dimensional precision translation stage. By moving it we can obtain a pair of PSFs with known defocus amount. A small amount of phase diversity can be introduced into the optical system through using the deformation mirror (DM).

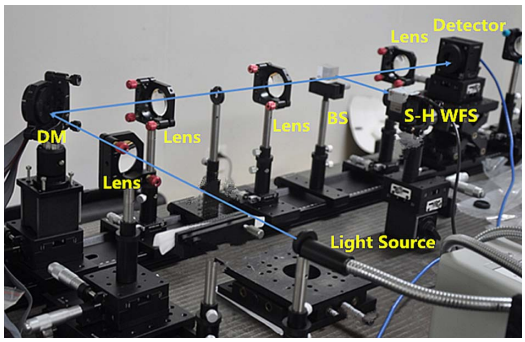

Fig. 8. Real facility of the optical system for PD.

Experimental parameters are set as follows: the focal length of the lens is 180 mm, the defocus distance is 1.5 mm, the wavelength is 632.8 nm, and the pixel size of the detector is 5500 nm.

The calculated Zernike coefficients by the VSACS and true Zernike coefficients measured by the Shack–Hartman wavefront sensors (S-H WFS) and the root mean square error of the coefficients calculated by Eq. (22) are shown in Table 4. This fact can qualitatively demonstrate the effectiveness of the modified algorithm.

The Zernike coefficients solved by the VSACS are used in this paper to reconstruct the defocus image and the focus image, which is the actual image acquisition for the experiment, and the reconstruction accuracy is evaluated by using the following Eq. (23) as the criterion [28,29]:

$$\sigma_{\mathrm{RMSE}} = \left\{ \frac{\sum_{i=1}^{M} \sum_{j=1}^{N} [\hat{o}(i,j) - o(i,j)]^2}{\sum_{i=1}^{M} \sum_{j=1}^{N} o(i,j)^2} \right\}^{1/2}. \tag{23}$$

$o(i,j)$ is the actual image acquisition for the experiment, and $\hat{o}(i,j)$ is the reconstruction image by the VSACS. The smaller the RMSE value is, the better the image reconstruction

Table 4. Calculated Zernike Coefficients by VSACS and True Zernike Coefficients Measured by the S-H WFS

	Case1		Case2		Case3	
Coefficient	Set	Calculated	Set	Calculated	Set	Calculated
a_5	−0.0943	−0.0934	0.0474	0.0480	−0.1064	−0.1015
a_6	−0.0215	−0.0281	−0.0803	−0.0800	−0.1917	−0.1961
a_7	−0.0018	−0.0020	0.0396	0.0444	0.1451	0.1425
a_8	1.1176	1.1018	0.3782	0.3644	0.7738	0.7520
a_9	−0.4244	−0.4368	−0.3286	−0.3191	0.0586	0.0577
a_{10}	0.1845	0.1781	0.1177	0.1172	0.1378	0.1331
a_{11}	−0.0390	−0.0374	−0.0312	−0.0297	0.0179	0.0187
a_{12}	0.0069	0.0087	0.0054	0.0061	0.0008	0.0010
a_{13}	−0.0013	−0.0009	0.0068	0.0008	0.0021	0.0015
a_{14}	−0.0034	−0.0022	0.0011	0.0013	0.0018	0.0023
RMSE (λ)	0.0071		0.0059		0.0074	

Table 5. Images Acquired Directly from Experiments and Images Reconstructed with the Zernike Coefficients Calculated by the Improved Cuckoo Search Algorithm and Reconstruction RMSE

	Defocus Image(a)	In-focus Image(a)	Defocus Image(b)	In-focus Image(b)	Defocus Image(c)	In-focus Image(c)
Directly collected images through experiments		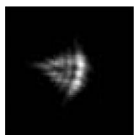			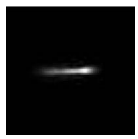	
Reconstruction image		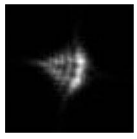				
Reconstruction RMSE	1.35%	2.26%	0.60%	0.47%	0.68%	1.04%

quality is, and the higher the accuracy of the phase diversity algorithm is.

Images acquired directly from experiments and images reconstructed with the Zernike coefficients calculated by the VSACS are shown in Table 5. In Table 5, the words "in-focus" and "defocus" mean only that the two images are collected at different focal planes. It can be seen from Table 5 that the maximum root mean square error value of the experimental image reconstructions is only 2.26%, which fully proves the effectiveness of the VSACS for PD.

6. CONCLUSION

The phase diversity algorithm will eventually be converted into a large-scale nonlinear numerical optimization problem. The choice of numerical optimization algorithm determines the accuracy and speed of the final aberration solution. We introduce the cuckoo search optimization algorithm into the phase diversity algorithm, and by optimizing the step size factor of the traditional cuckoo search algorithm, the convergence speed of the cuckoo search algorithm for PD is accelerated. A large number of simulations are used to prove the effectiveness of this optimization algorithm for PD. Especially in the case of large-scale dimension of optimization variables, the convergence rate and accuracy of the VSACS algorithm for PD are higher than the traditional PSO for PD under the different conditions. Finally, we verified the effectiveness of VSACS for PD through a simple experiment.

Funding. National Natural Science Foundation of China (NSFC) (11703027).

REFERENCES

1. J. A. Koch, R. W. Presta, R. A. Sacks, R. A. Zacharias, E. S. Bliss, M. J. Dailey, M. Feldman, A. A. Grey, F. R. Holdener, J. T. Salmon, L. G. Seppala, J. S. Toeppen, L. Van Atta, B. M. Van Wonterghem, W. T. Whistler, S. E. Winters, and B. W. Woods, "Experimental comparison of a Shack-Hartmann sensor and a phase-shifting interferometer for large-optics metrology applications," Appl. Opt. **39**, 4540–4546 (2000).
2. M. J. Booth, "Adaptive optical microscopy: the ongoing quest for a perfect image," Light Sci. Appl. **3**, e165 (2014).
3. F. Roddier, "Curvature sensing and compensation: a new concept in adaptive optics," Appl. Opt. **27**, 1223–1225 (1988).
4. S. Esposito, E. Pinna, A. Tozzi, P. Stefanini, and N. Devaney, "Cophasing of segmented mirrors using the pyramid sensor," Proc. SPIE **5169**, 72–79 (2003).
5. X. Rondeau, E. Thiébaut, M. Tallon, and R. Foy, "Phase retrieval from speckle images," J. Opt. Soc. Am. A **24**, 3354–3365 (2007).
6. A. C. Sobieranski, F. Inci, H. C. Tekin, M. Yuksekkaya, E. Comunello, D. Cobra, A. von Wangenheim, and U. Demirci, "Portable lensless wide-field microscopy imaging platform based on digital inline holography and multi-frame pixel super-resolution," Light Sci. Appl. **4**, e346 (2015).
7. R. G. Paxman, B. J. Thelen, and J. H. Seldin, "Phase-diversity correction of turbulence-induced space-variant blur," Opt. Lett. **19**, 1231–1233 (1994).
8. V. Korkiakoski, C. Keller, N. Doelman, R. Fraanje, and M. Verhaegen, "Joint-optimization of phase-diversity and adaptive optics," in *Imaging and Applied Optics* (Optical Society of America, 2011), paper JTuC5.
9. I. Klapp and J. Rosen, "Phase diversity implementation in Fresnel incoherent holography," in *Imaging and Applied Optics* (Optical Society of America, 2013), paper CTh3C.3.
10. D. J. Lee, B. M. Welsh, M. C. Roggemann, and B. L. Ellerbroek, "Diagnosing unknown aberrations in an adaptive optics system by use of phase diversity," Opt. Lett. **22**, 952–954 (1997).
11. P. G. Zhang, C. L. Yang, Z. H. Xu, Z. L. Cao, Q. Q. Mu, and L. Xuan, "Hybrid particle swarm global optimization algorithm for phase diversity phase retrieval," Opt. Express **24**, 25704–25717 (2016).
12. J. R. P. Angel, P. Wizinowich, M. Lloyd-Hart, and D. Sandler, "Adaptive optics for array telescopes using neural-network techniques," Nature **348**, 221–224 (1990).
13. Y. Rivenson, Y. Zhang, H. Günaydın, D. Teng, and A. Ozcan, "Phase recovery and holographic image reconstruction using deep learning in neural networks," Light Sci. Appl. **7**, 17141 (2018).
14. H. Y. Y. Li, "Genetic algorithm for phase retrieval of generalized phase diversity," Energy Procedia **13**, 4806–4811 (2011).
15. P. M. Johnson, M. E. Goda, and V. L. Gamiz, "Multiframe phase-diversity algorithm for active imaging," J. Opt. Soc. Am. A **24**, 1894–1900 (2007).
16. X. S. Yang and D. Suash, "Cuckoo search via Lévy flights," in *World Congress on Nature & Biologically Inspired Computing (NaBIC)* (2009), pp. 210–214.
17. X.-S. Yang and S. Deb, "Multiobjective cuckoo search for design optimization," Comput. Oper. Res. **40**, 1616–1624 (2013).
18. X.-S. Yang and S. Deb, "Engineering optimisation by cuckoo search," Int. J. Math. Model. Numer. Optim. **1**, 330–343 (2010).
19. R. A. Gonsalves, "Phase retrieval and diversity in adaptive optics," Opt. Eng. **21**, 215829 (1982).
20. R. J. Noll, "Zernike polynomials and atmospheric turbulence*," J. Opt. Soc. Am. **66**, 207–211 (1976).
21. H. Akaike, "Information theory and an extension of the maximum likelihood principle," in *Selected Papers of Hirotugu Akaike*, E. Parzen, K. Tanabe, and G. Kitagawa, eds. (Springer, 1998), pp. 199–213.
22. X.-S. Yang, *Nature-Inspired Metaheuristic Algorithms* (Luniver, 2008).
23. M.-L. Gao, L.-J. Yin, G.-F. Zou, H.-T. Li, and W. Liu, "Visual tracking method based on cuckoo search algorithm," Opt. Eng. **54**, 073105 (2015).
24. H. Zhuang and Z. Roth, "Method for kinematic calibration of Stewart platforms," J. Robot. Syst. **10**, 391–405 (1993).
25. X.-S. Yang and S. Deb, "Cuckoo search: recent advances and applications," Neural Comput. Appl. **24**, 169–174 (2014).
26. M. Clerc, "The swarm and the queen: towards a deterministic and adaptive particle swarm optimization," in *Evolutionary Computation (CEC)* (IEEE, 1999), pp. 1951–1957.
27. I. C. Trelea, "The particle swarm optimization algorithm: convergence analysis and parameter selection," Inf. Process. Lett. **85**, 317–325 (2003).
28. X. Qi, G. Ju, and S. Xu, "Efficient solution to the stagnation problem of the particle swarm optimization algorithm for phase diversity," Appl. Opt. **57**, 2747–2757 (2018).
29. W. Zhou, A. C. Bovik, H. R. Sheikh, and E. P. Simoncelli, "Image quality assessment: from error visibility to structural similarity," IEEE Trans. Image Process. **13**, 600–612 (2004).